






Original Article

Correlation between ore mineralogical composition at different depths and Bond Work Index for the Erdenetiin Ovoo Cu-Mo porphyry deposit, Mongolia

Batmunkh Tumen-Ayush^{1,2} , Chinzorig Bavuu², Narangerel Adiyasuren¹, Davaajargal Darambazar³, Ganbileg Davaajav³, Khaliun Amartuvshin³, Sondor Ganbat³, Tsend-Ayush Tserendagva¹, Altankhuyag Dorjyunden¹ , Ganzorig Chimed^{3*} 

¹Erdenet Mining Corporation SOE, Orkhon province, Erdenet 61027, Mongolia

²Department of Mining Technology, School of Geology and Mining Engineering, Mongolian University of Science and Technology, Ulaanbaatar 14191, Mongolia

³Center for Nanoscience and Nanotechnology, Department of Chemical and Biological Engineering, School of Engineering and Technology, National University of Mongolia, Ulaanbaatar 14201, Mongolia

*Corresponding author: ch_ganzorig@num.edu.mn, ORCID: 0000-0003-3807-7743

ARTICLE INFO

Article history:

Received: 18 September, 2024

Revised: 23 January, 2025

Accepted: 07 February, 2025

ABSTRACT

The Erdenetiin Ovoo Cu-Mo porphyry deposit in Mongolia is the largest copper mine corporation in the nation. In this study, we investigate the grinding properties of biotite granodiorite and granodiorite rock alteration relative to variations in mine depth, with a specific focus on their correlation with mineral composition. The Bond Work Index experimental tests are applied to the Cu-Mo porphyry ore from the Erdenet Mining Corporation in Mongolia. The samples used in this study were collected representing 10 composites of 5 different depth levels with an interval of ~90 m within the 1175-725 m sampling elevation. The chemical, surface analytical, and mineralogical characterizations of the two types of biotite granodiorite and granodiorite ores are performed using Inductively Coupled Plasma, X-ray fluorescence, and X-ray diffractometer methods. Results of the chemical analysis indicate that the Cu and Mo percentages of both biotite granodiorite and granodiorite consistently decreased with depth profiling. The X-ray diffractometer data of mineral composition are used in setting up the prediction of the Bond Work Index estimation model. An equation-based approach to the Bond Work Index estimation model demonstrates a strong linear correlation ($R^2=0.895$) with the measured Bond Work Index from experimental tests, with the highest Bond Work Index measured at 19.06 kWh/t. Our experimental results indicate that strong correlations were identified between the major mineral phases and the Bond Work Index values through the integration of ore hardness and mineralogical data.

Keywords: ore hardness, estimation model, biotite granodiorite, granodiorite, mineralogy

INTRODUCTION

A geometallurgical correlation inherently links the characteristics of the rock, including mineralogy, texture, geochemistry, and physio-mechanical properties, to its processing behavior (Dominy et al., 2018). Therefore, it is predicted that these variations may influence a beneficiation plant's main processing parameters throughput

and recovery in a negative way (Frenzel et al., 2023). A well-known parameter influencing the performance of a comminution circuit, mainly throughput, is grindability, which is defined as an ore's resistance to breakage (Varianemil et al., 2023; Shi et al., 2009).

In the mineral industry, the essential requirement for all subsequent separation or extraction

undertakings involves the liberation of valuable minerals from gangue. This paramount goal is actualized through a series of rock fragmentation stages, accomplished through ore comminution. Intriguingly, the empirical Bond Work Index (BWI) typically governs the assessment of crushing energy in the mineral processing sector, irrespective of a rock's mechanical attributes (Bhukte et al., 2023).

The complexity of ore mineralogy is a challenge for the mining industry. In particular, within the same ore body, there can be a variety of mineralization zones (with different minerals) for which different process flow sheets (Kalichini et al., 2017; Lessard et al., 2016; Paquot et al., 2015). Process mineralogy, the practical application of mineralogy to assist process plant design (Bradshaw, 2014; Whiteman et al., 2016), has been used in mineral processing to understand how mineralogical data can be used to predict and understand the behavior of ores when subjected to comminution (Parker et al., 2015; Kingman et al., 2004) and separation and recovery processes (Zhou et al., 2021; Solomon et al., 2011).

Most of the research works reported in the literature provide information about the grindability and crushing energy of rock (Nghipulile et al., 2022; García et al., 2021). However, to the best of our knowledge, no studies have been reported on the correlation between ore mineralogy and grindability with respect to varying mine depths in a downward direction. Thus, our research work addresses the relationship between the mineralization of ore and the BWI, specifically for an Erdenetiin Ovoo Cu-Mo porphyry ore.

The grinding properties and strength attributes of rocks are contingent upon the content of constituent rock-forming minerals and their specific alteration patterns, thus prompting an exploration of their correlation with the mineral composition values within the experimental dataset.

Thus, our research objective is to investigate the grinding properties of biotite granodiorite (BGDP) and granodiorite (GDIR) rock alteration relative to variations in mine depth levels, with a specific focus on their correlation with mineral composition in the selected samples.

The relationship between the mineralization of ore and the BWI, specifically for the Northwest deposits of Erdenetiin Ovoo Cu-Mo porphyry ore is also investigated in this work.

MATERIALS AND METHODS

Regional geology of Erdenetiin Ovoo Cu-Mo porphyry deposit

Erdenet Mining Corporation, about 350 km Northwest of the capital city of Ulaanbaatar, mines the Erdenetiin Ovoo Cu-Mo porphyry deposit, one of the largest copper-molybdenum deposits in Mongolia. The deposit is hosted by an intrusive complex in the Orkhon-Selenge trough (Sarantsatsral et al., 2021).

The mine, which started operations in 1978, splits the mining area primarily into four deposits, Central, Northwest, Shand, and Oyut. The Erdenetiin Ovoo Cu-Mo porphyry deposit is hosted by a late Permian to early Triassic intrusive complex Fig. 1, which forms part of the extensional volcano-plutonic belt within the Orkhon-Selenge trough (Gerel et al., 2005). The orebody of the Erdenetiin Ovoo Cu-Mo porphyry deposit extends over an area of 2×1 km, with a maximum vertical thickness of 560 m, including a 100 to 300 m thick secondary Cu-enriched supergene zone at the top (Haruhisa, 2003).

The Erdenet Porphyry Complex consists of diorite and granodiorite porphyry, divided into three stages: (1) diorite porphyry and micro-diorite, (2) granodiorite porphyry, and (3) granodiorite associated with breccia (Dejidmaa and Kazuki, 1998).

Granodiorite, a coarse-grained rock, primarily consists of quartz, plagioclase feldspar, and a lesser amount of potassium feldspar. Its appearance often exhibits a salt-and-pepper texture due to the intermingling of dark-colored minerals like biotite and hornblende. The presence of plagioclase feldspar imparts a characteristic gray to light gray color to granodiorite.

Biotite granodiorite, as the name implies, contains significant amounts of biotite, a dark-colored mica mineral. Biotite contributes to the darker tone observed in this rock type, spanning a range of hues. The occurrence of granodiorite and biotite granodiorite in the Erdenet mining

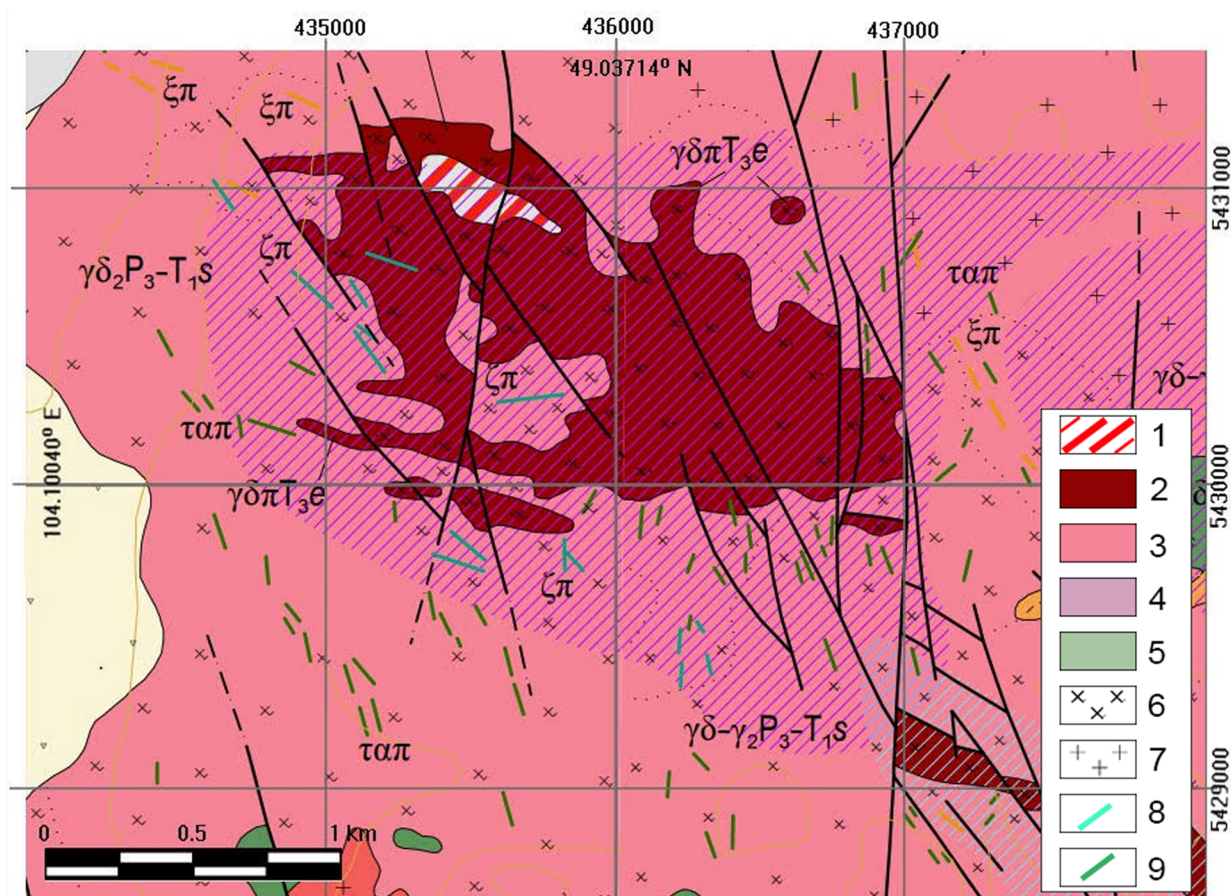


Fig. 1. Geological map of the Erdenetiin Ovoo Cu-Mo porphyry deposit. The Selenge Complex: 1-felsite; 2,6-diorite porphyry, granodiorite porphyry; 3-granodiorite; Erdenet Porphyry Complex: 4-andesite; 5-felsite; 7-granosyenite; 8-monzodiorite porphyry; 9-andesite and trachyandesite porphyry

district can be attributed to the area’s tectonic history.

Sample selection

The sampling campaign for the Northwest (NW) was determined based on the logged lithological unit from the Erdenet Mining Corporation mine database and the main alteration minerals observed. A total of 66 samples were collected for this study, representing different lithology and alteration zones within the Erdenetiin Ovoo Cu-Mo porphyry deposit. The samples were collected representing 10 composites of 5 different levels with an interval of 90 m

within the 1175-725 m sampling elevation. The sampling elevations of the BGDP and GDIR as the rock types of the samples are shown in Table 1.

Samples were procured employing conventional diamond drilling techniques, featuring a core diameter measuring 65 mm. Following extraction, the core underwent segmentation into 1 m segments, with half of each segment reserved for subsequent analysis. Fig. 2 shows two views of the drill holes. Some holes were drilled from the surface before the start of operations, while other holes were drilled inside the pit.

Table 1. Elevation of the collected samples

Level of depth	Elevation, m	Rock type	
		BGDP	GDIR
L1	1175 - 1085	L1_BG	L1_GD
L2	1085 - 995	L2_BG	L2_GD
L3	995 - 905	L3_BG	L3_GD
L4	905 - 815	L4_BG	L4_GD
L5	815 - 725	L5_BG	L5_GD

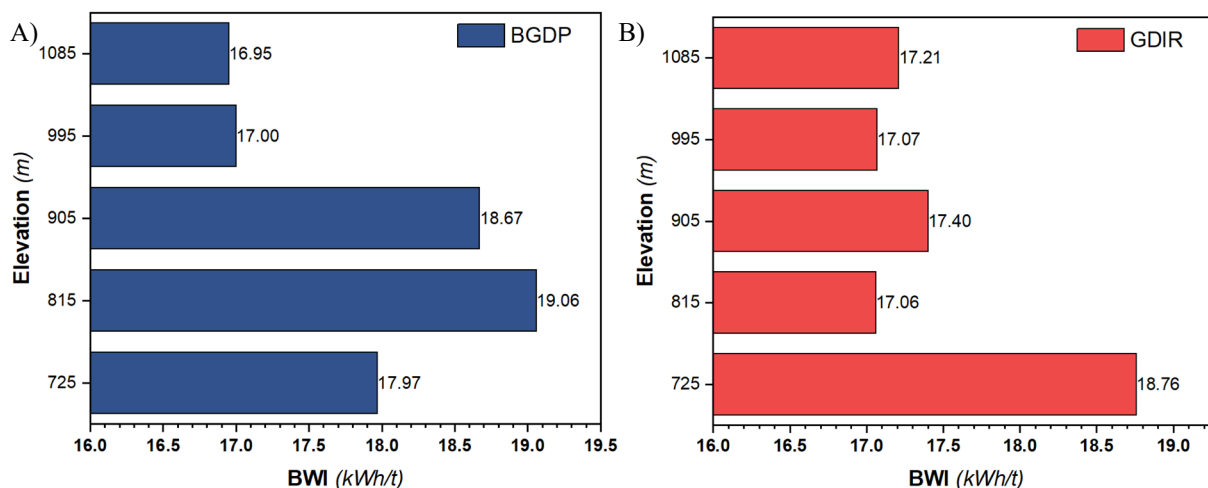


Fig. 2. Comparison of BWI value and mine depth in a downward direction; A) BGDP rock; B) GDIR rock.

Bond Ball Mill test

The Bond ball mill work index (BWI) is obtained from the Bond Ball Mill test, a locked-cycle laboratory test that measures the ball mill grinding energy required for a given ore throughput. It indicates ore resistance and breakage characteristics on the micron scale.

BWI tests are conducted at the Erdenetiin Ovoo mine laboratory using a standard Bond ball mill and test methodology. The feed is prepared by compositing fractions of core segments from the sample interval within 90 m after initial crushing to -3.36 mm. The composite feed is then ground to 80% passing a product size of 150 microns. For the first test, samples finer than -3.36 mm were prepared via jaw crusher. From there, 700 ml of the material is placed in the mill and ground dry, with a 250 percent circulating load. The grinding process occurs in cycles with periodic screening of the material on sieves of different mesh sizes. Fresh unsegregated feed is added to the oversize to maintain the original charge weight. The number of revolutions for each grinding period is calculated to achieve a 250 percent circulating load, targeting a sieve undersize equal to $1/3.5$ of the total charge in the mill.

This procedure was systematically repeated until a consistent set of two or three grindability values emerged. This process continues until a stable equilibrium is reached in terms of the net grams of sieve undersize produced per mill revolution. Finally, the ground product of the last test was sieved to determine (P80). The average of the last three net grams per

revolution determines the Ball Mill Grindability (Magdalinovic, 1989; Ahmadi and Shahsavari, 2009; Todorovic et al., 2017).

Chemical and mineralogical analysis

Chemical analysis (XRF and ICP)

X-ray fluorescence (XRF) in the model of PANalytical's MiniPal-4 was performed on the samples to determine copper, molybdenum, and Iron content. In order to conduct a comprehensive analysis of the elemental composition in minerals, we prepared the collected sample preparation involving reduction to a particle size of less than $3 \mu\text{m}$.

Furthermore, the elemental composition analysis was conducted using the Inductively Coupled Plasma (ICP) method, which allows accurate determination of constituent elements. The analysis detected elements from sodium to antimony using their K lines of X-ray spectrum. The total elemental compositions were accurate to one part in one million after calibrating with standard samples. A total of 31 elements from 10 composite samples were analyzed for this experiment, including valuable elements - Cu, Mo; penalty elements - Pb, As, P, etc.; and copper phases - Cu (I), Cu (II), and CuO.

Mineralogical characterization (XRD)

The samples were initially prepared as a fine with a size of $<75 \mu\text{m}$, and $>10 \mu\text{m}$ then ground until $3 \mu\text{m}$ with XRD-Mill McCrone, a lab miller, and analyzed with X-ray Powder Diffraction Analysis and Rietveld Quantitative Phase Analysis techniques. X-ray diffraction

(XRD) instrument manufactured by Analytical X-ray Company was utilized to define the chemical composition of the minerals. In total, the instrument determined a weight percentage of 34 minerals present in each composite sample.

XRD analysis provided detailed mineralogical insights, while XRF and ICP analysis provided a solid profile of elemental composition. In essence, these methodological approaches laid the foundation for a broad understanding of the sample's characteristics and properties and ensured a comprehensive analysis of samples.

RESULTS AND DISCUSSION

Bond ball index test results

The result of the BWI test for both BGD and GDIR rock samples in relation to mine depth is shown in Fig. 3. For BGD rocks, the hardness of the ore increases significantly and changes to 19.1 kWh/t when the mine depth level falls below 995 m, and further reduces while the elevation falls below 800 m in Fig. 3. However, as the mine depth decreased for GDIR rock, less change was determined, and the average hardness of ore in the elevation range from 815 m to 725 m increased drastically from 17.22 to 18.76 kWh/t.

Table 2. Grinding time of two lithologies

Level	Depth, m	Grinding time, P80					
		(Note: The -75 μm class is 58-62% in flotation feed)					
		BGD	15 min	20 min	GDIR	15 min	20 min
L1	1175 -1085	L1_BG	113.95	90.62	L1_GD	119.79	95.00
L2	1085 -995	L2_BG	109.84	88.37	L2_GD	113.71	90.17
L3	995 - 905	L3_BG	122.67	96.77	L3_GD	110.22	86.06
L4	905 - 815	L4_BG	126.90	101.62	L4_GD	115.41	97.18
L5	815 - 725	L5_BG	129.42	96.86	L5_GD	127.12	99.57

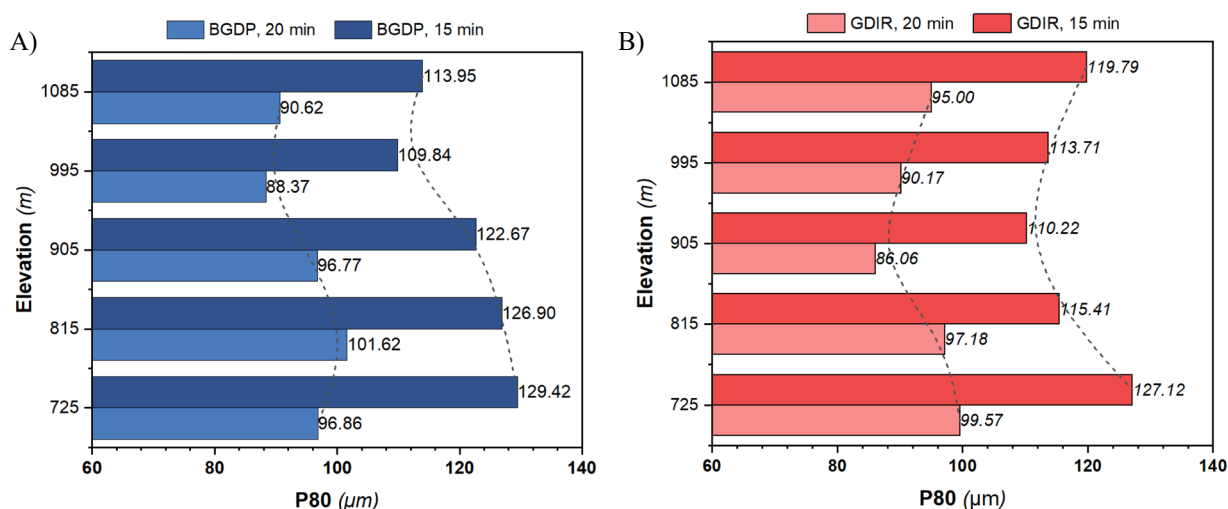


Fig. 3. Variation of grinding time for A) BGD rock, and B) GDIR as a function of mining depth

Table 3. Copper and molybdenum concentration for the two types of ore

Level of depth	Elevation, m	Rock type			
		BGD		GDIR	
		Cu, %	Mo, %	Cu, %	Mo, %
L1	1175 - 1085	0.362	0.013	0.282	0.015
L2	1085 -995	0.343	0.010	0.380	0.026
L3	995 - 905	0.276	0.024	0.343	0.012
L4	905 - 815	0.248	0.019	0.283	0.012
L5	815 - 725	0.285	0.012	0.245	0.011

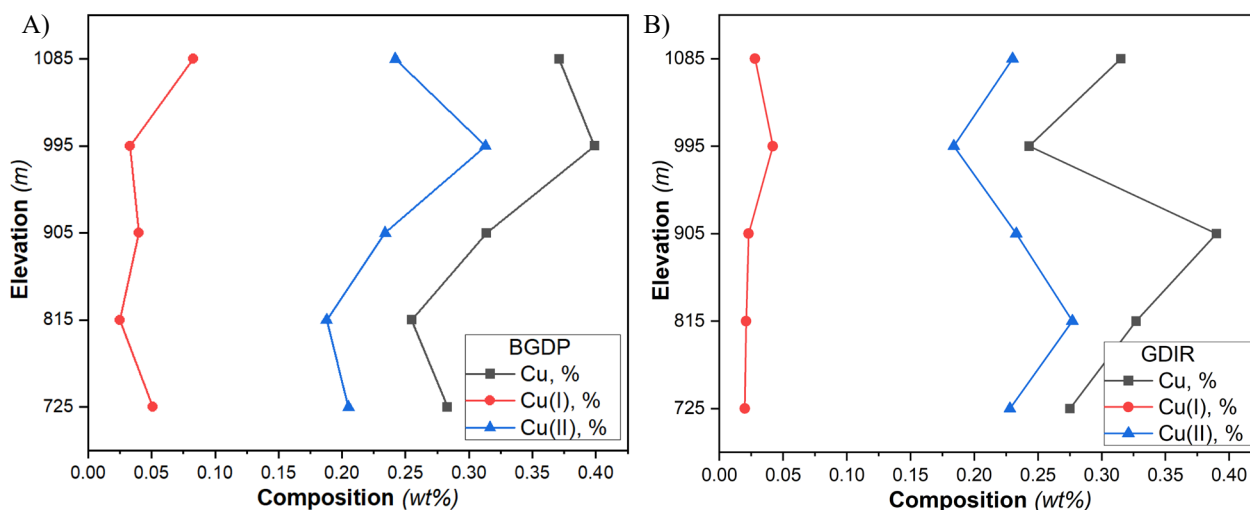


Fig. 4. Variation in the content of copper (Cu%), primary copper (chalcopyrite), and secondary copper across different depth levels of A) BGDP and B) GDIR

Variation in grinding time data for two lithologies (BGDP and GDIR) across different depth levels is shown in Table 2 and Fig. 4. The grinding time data consists of two times, 15 minutes and 20 minutes, with the corresponding P80 values. P80 values for BGDP seem to be generally higher than GDIR for both grinding times. For both lithologies, grinding for 20 minutes consistently results in lower P80 values compared to 15 minutes, indicating a finer grind.

The higher P80 values observed, especially for BGDP, also hint at a more challenging grindability, implying that the rock ore is harder. This observation aligns well with the principles of the BWI, further validating its relevance and applicability in assessing the hardness and grindability of the lithologies in question.

Chemical and mineralogical characterization

The chemical composition of the BGDP and GDIR rock composite samples for Cu and Mo content are presented in Table 3. In the “X-ray Spectrum Laboratory”, elemental composition determination (XRF) analysis was conducted on 36 sets of samples from 5 levels. The chemical characterization is to explore how the content of copper (Cu) and molybdenum (Mo) changes depending on the type of rock as the mine level gets lowered (L1-L5).

The copper percentages of both BGDP and GDIR consistently decrease with depth. Table 3 shows the results of the elemental composition analysis of biotite-granodiorite (BGDP) rock.

At the level of 1175-1085 m, the copper and molybdenum contents were 0.362% and 0.013%, respectively. However, at the level of 725 m, a decrease in copper and molybdenum content to 0.258% and 0.008% was observed. And accrued for the L5, but Cu shares fall to other levels.

For GDIR rocks, the copper and molybdenum contents were 0.282% and 0.015%, respectively, at the level of 1175-1085 m. It is worth noting that the copper, molybdenum, and iron contents of both the BGDP and GDIR rocks are similar. In GDIR, there’s the highest value or 0.38% in copper percentages at the depth of 1085-995 m, after which it decreases.

The results show that the content of II-valent copper (Cu-II%) and copper (Cu%) decreases as the level of BGDP rocks decreases. However, the L2 and L5 levels have a higher content of copper, I-valent copper, and II-valent copper than the other samples.

The chemical analysis of GDIR rocks showed that the contents of single copper, 1-valent copper, and 2-valent copper were similar in each batch as the depth level of the borehole decreased. However, the L2 level had a higher content of these metals than the other sets of samples Fig. 4B.

Correlation between mineral composition and BWI

To investigate the mineral composition of the Erdenetiin Ovoo Cu-Mo porphyry deposit

Table 4. Mineral composition at varying depths in BGD and GDIR rocks

Minerals and Chemical composition	Pearson correlation coefficient with BWi	Rock type									
		BGDP					GDIR				
		L1	L2	L3	L4	L5	L1	L2	L3	L4	L5
Albite	0.818	28.5	29.3	31.6	36.7	33.2	32.1	28.8	28.3	31.6	35.2
Andradite	0.058	0.4	0.4	0.3	0.6	0.2	0.5	0.3	0.4	0.2	0.2
Ankerite	-0.079	0.9	0.2	0.4	0.4	0.6	0.2	0.3	0.2	0.2	0.1
Anorthite	-0.309	1.6	1.3	1.2	1.3	0.4	2.0	1.1	0.8	1.6	1.1
Bornite	-0.214	0	0	0	0	0	0.1	0	0	0	0
Calcite	0.509	0	0.6	1.1	0.5	0.6	0.8	0.4	0.7	0.9	1.5
Chalcopyrite	-0.685	0.9	1.1	0.8	0.6	0.8	0.7	1	1	0.8	0.7
Chlorite	0.213	1.1	1.2	1.7	1.9	1.2	2.8	1.9	1.1	2.2	2.5
Covellite	-0.144	0.1	0	0	0	0.3	0.1	0.2	0.1	0	0.1
Dickite	0.227	0.2	0.2	0.4	0.3	0.9	0.1	0.4	0.3	0.4	0.3
Diopside	0.314	0.2	0.4	0.4	0.4	0.3	0.7	0.2	0.1	0	0.4
Gypsum	0.457	0.8	1.3	0.7	0.8	0.3	0.7	1.0	1	0.7	0.6
Hematite	-0.013	0.2	0.1	0.2	0.4	0.1	0.4	0.3	0.1	0.1	0.4
Kaolinite	0.447	1.0	0.5	0.6	0.3	0.8	0.3	0.3	0.5	0	0.4
Laumontite	0.115	0.8	1.1	1.5	1.7	1.7	0.9	2.1	1.1	1.5	1.7
Malachite	0.199	0	0	0	0	0.2	0	0	0.2	0.4	0.4
Microcline	-0.449	1.9	2.3	3.1	2.8	4.0	3.4	4.0	3	2.5	3.1
Molybdenite	0.108	0.1	0	0	0	0	0	0.1	0	0	0
Muscovite	0.518	21.6	20.7	18.3	14.7	16.4	17.6	19.3	21	17.1	17
Orthoclase	0.028	3.4	2.6	3.3	6.2	3.9	3.5	3.6	2.4	4.8	4.0
Prehnite	-0.865	0.3	0.6	0.7	0.5	1.4	0.4	1.5	0.9	1.3	1.3
Pyrite	-0.620	1.7	1.4	1.0	0.2	1.0	1.4	1.4	1.5	1.1	0.8
Quartz	0.818	33.1	33.4	31.7	28.0	30	29.8	29.9	34.2	30.9	26.7

changes with depth, we used an XRD to determine the mineral composition of samples from the L1-L5 levels with BGD and GDIR rock types. The results are shown in Table 4.

The analysis of BGD rock samples from boreholes L1-L5 shows that the albite content is high in the L1-L4 level (1175-815 m) but decreases in the L5 level (815-725 m). Andradite content increases between 1175-995 m and 905-815 m while L3 and L5 decrease. Ankerite, a dolomite group mineral, is usually found in sulfide deposits and has the highest content of 0.9 in the L1 (1175-1085 m) sample, and the lowest content in the L5 (815-725 m) sample. The mineral content of the hard minerals calcite and microcline increased in the L2 level, while it decreased in the other samples. The mineral content of chlorite, diopside, and laumontite increased in the L1 level, while it decreased in the other levels. Orthoclase and hematite, which

are also hard minerals, had increased mineral content in the L1, L3, and L4 levels. Covellite, muscovite, and pyrite increased in the L2-L4 levels but decreased in the L1 and L5 levels.

According to the results of XRD analysis of GDIR rock samples, the minerals covellite, gypsum, muscovite, prehnite, and pyrite decreased in the depth of 905-725 m, while their content increased at L2 and 1085-995 m, respectively. For andradite and diopside, the mineral content decreased at the L2-L5 level. Chalcopyrite and orthoclase increased in the L5 level and decreased in the other depths.

In Table 4, the mineral composition, as determined by XRD is correlated with the BWI using Pearson's method. When applying Pearson's correlation, it's important to note specific assumptions. The correlation coefficient lies between -1 and 1, indicating positive, negative, or no correlation, respectively.

An equation-based approach to BWI estimation model

Pearson correlation coefficient between the BWI test results and the XRD results of significant mineral compositions are shown in Table 5.

The Pearson Correlation Coefficient values help in understanding the relationship intensity between mineral composition and BWI values. High correlation values (closer to 1) indicate that the mineral's presence has a more pronounced impact on the BWI, while values closer to 0 suggest a weaker relationship (Adler and Parmryd, 2010).

In this study, the mineral compositions showed different correlations with the BWI. Pyrite showed the most significant negative correlation (-0.865), indicating that the value probably decreases with increasing concentration. Similarly, muscovite (-0.676) and quartz (-0.620) also showed a negative relationship with BWI, suggesting that their increased composition might decrease BWI. In contrast, albite (0.818) and orthoclase (0.518) had positive correlations, suggesting that their increasing concentrations could elevate the BWI. Microcline, with a correlation of 0.199, indicates a comparatively weaker positive association with BWI.

Minerals related to pyrite and muscovite show negative correlations, indicating they may inversely influence BWI, while albite and orthoclase demonstrate positive correlations, suggesting they may have a proportional impact on BWI. These results suggest that mineral composition values can be used in multilinear equation models to calculate the BWI.

Fig. 5A and Fig. 5B show the mineral compositions of quartz, albite, and muscovite at different depths for both lithologies. In BGD, Quartz composition generally decreases as we

go deeper, with a few variations. Albite seems to increase in composition as depth increases, reaching a peak at 815 m, after which it starts to decrease. Muscovite has a decreasing trend with increasing depth. In GDIR, the compositions of Quartz and Albite seem to fluctuate, but Albite maintains a higher composition in the deeper depths. Muscovite also shows a declining trend similar to BGD.

Fig. 5C and Fig. 5D indicate the mineral compositions of orthoclase, microcline, and pyrite across different depths. In BGD, orthoclase exhibits fluctuations, peaking notably at 815 m, while microcline's presence rises, peaking at 725 m. Pyrite remains relatively stable, except for a pronounced dip at 815 m. Microcline maintains a relatively consistent distribution with a slight decrease at 815 m, and Pyrite generally diminishes as depth segments.

The scatter plots illustrate the correlation between the BWI and mineral content in Fig. 6. Fig. 6A, clearly shows that the ascending order of values is associated with a decrease in quartz and muscovite content. Albite, which exhibits the highest positive Pearson's correlation coefficient of 0.623, demonstrates a substantially prominent increase in mineral composition as the BWI values ascend.

Fig. 6B indicates that minerals exhibit weak correlation coefficients (>0.3) despite a rise in composition (Saxena et al., 2024). Notably, even though the mineral composition increases, the percentage remains lower.

Testing methodology for the BWI requires about 10 kg of sample, the standardized equipment, and takes an average of 6 to 12 hours. Many researchers have tried to find alternative methods for determining this Index to reduce labor costs, and sample weight, or to get one without standard equipment (Shi et

Table 5. Pearson correlation coefficient of BWI test result compared to XRD result of most significant mineral composition

Minerals	BWI, kWh/t	Quartz	Albite	Muscovite	Orthoclase	Microcline	Pyrite
BWI	1.00						
Quartz	-0.62	1.00					
Albite	0.82	-0.84	1.00				
Muscovite	-0.68	0.82	-0.92	1.00			
Orthoclase	0.52	-0.69	0.78	-0.83	1.00		
Microcline	0.20	-0.43	0.19	-0.39	0.01	1.00	
Pyrite	-0.86	0.72	-0.92	0.88	-0.82	-0.16	1.00
Other Minerals	0.24	-0.84	0.49	-0.60	0.42	0.58	-0.37

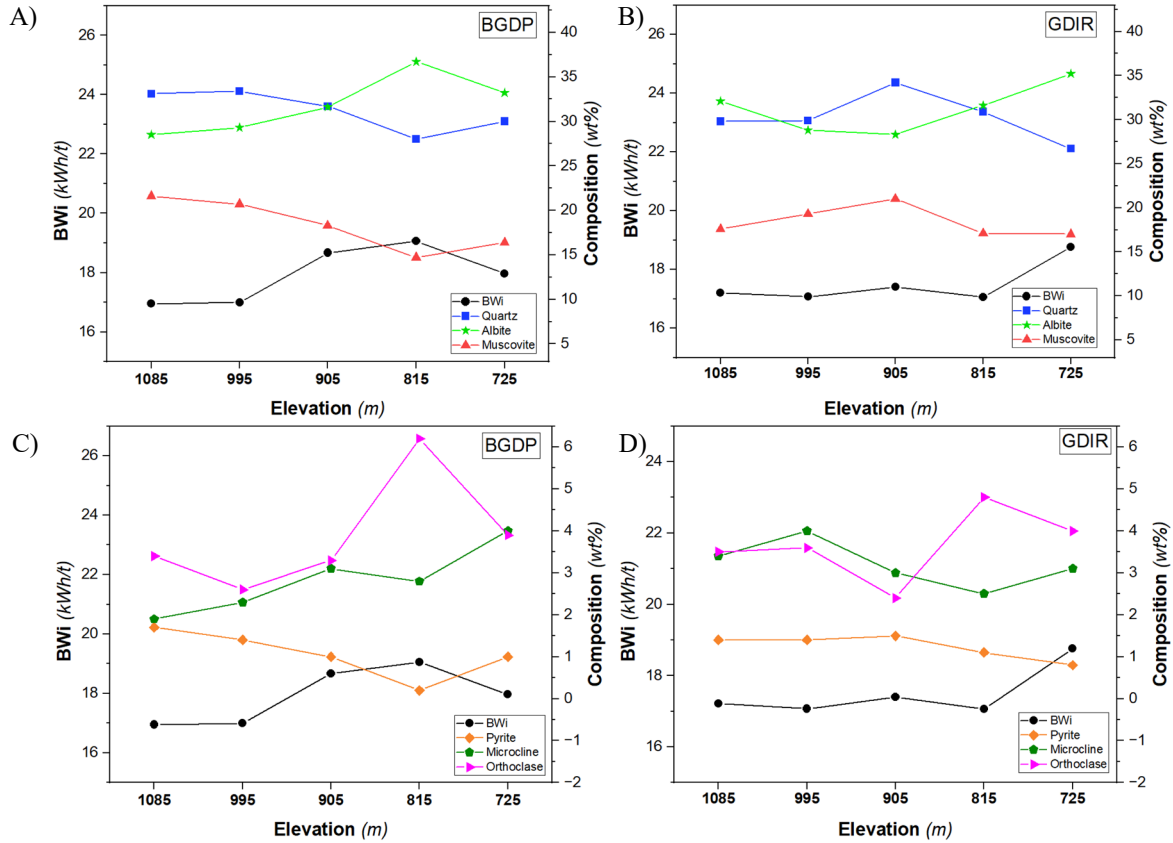


Fig. 5. Comparative mineral compositions at varying depths in BGDP and GDIR, as follows: A) and B) focus on quartz, albite, and muscovite, while C) and D) highlight orthoclase, microcline, and pyrite

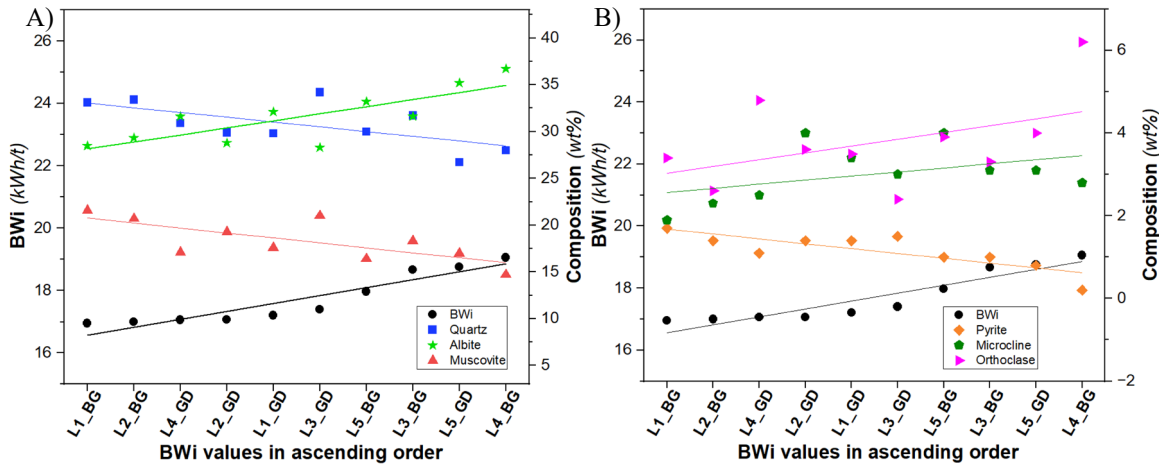


Fig. 6. Mineral compositions are as follows: A) quartz, albite, and muscovite, and B) orthoclase, microcline, and pyrite, in ascending order based on their bond work index

al., 2009). These researchers have employed multiple linear regression, using factors like chemical assays, modal mineralogy, lithology, and alteration. Keeney, et al. (2011) have developed models predicting the BWi for two distinct classes, with prediction errors of 7.4% ($R^2=0.84$) and 2.1% ($R^2=0.83$) for each class, respectively (Al-Tigani et al., 2020). However, these predictions are specific to a particular deposit. Hunt et al. (2013) also used multiple linear regression for modeling and highlighted

the effect of lithologies on correlations (Hunt et al., 2013).

In this study, we utilized the XRD composition values of muscovite, orthoclase, microcline, pyrite, albite, and quartz to develop a multilinear equation model for estimating the BWi, as shown in (Eq. 1). We determined the BWi for 10 samples from two distinct lithologies: biotite-granodiorite and granodiorite. However, due to a limited number of measured values, we created a single model for both lithologies.

$$BWi[kWh/t] = -0.0079 + 0.0619 \cdot \text{Quartz} (\%) + 0.3128 \cdot \text{Albite} (\%) + 0.3966 \cdot \text{Muscovite} (\%) - 0.0886 \cdot \text{Orthoclase} (\%) + 0.4089 \cdot \text{Microcline} (\%) - 1.8704 \cdot \text{Pyrite} (\%) - 0.0065 \cdot \text{Other Minerals} (\%) \quad (\text{Eq. 1})$$

Table 6. Measured and estimated value for BWI

Sample ID	Measured BWI, kWh/t	Estimated BWI, kWh/t	Residuals, kWh/t
L1_BG	16.95	16.75	-0.195
L2_BG	17.00	17.46	0.459
L3_BG	18.67	18.13	-0.540
L4_BG	19.06	19.18	0.123
L5_BG	17.97	18.08	0.113
L1_GD	17.21	17.24	0.030
L2_GD	17.07	17.12	0.050
L3_GD	17.04	17.44	0.036
L4_GD	17.06	17.03	-0.027
L5_GD	18.76	18.73	-0.031

Table 6 presents both the experimentally measured and estimated using the equation for bond index value. It also highlights the differences between these measured and estimated values. An equation-based approach to BWI, Fig. 6 shows the plot of estimated and measured BWI. Fig. 7 shows that a linear correlation exists between estimated and measured BWI ($R^2=0.895$).

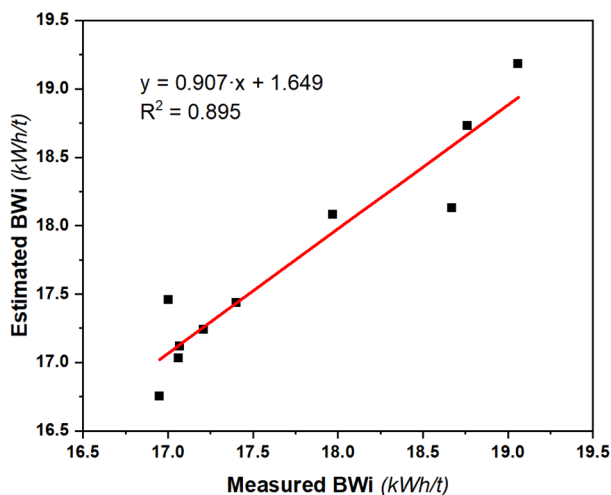


Fig. 7. Correlation between estimated and measured BWI

CONCLUSIONS

The aim of this study was to establish whether the variation in the mineralogical composition of biotite granodiorite and granodiorite rocks from Erdenetiin Ovoo porphyry deposit had an effect on their hardness value (BWI) when the mining operation level decreased which can, in turn, have implications on the future milling circuit design. The determination of the correlation between the values of modal mineralogy and

BWI was carried out using “The Pearson correlation coefficient” since the grindability of the ore depends on ore mineralogy and characteristics. According to this study, the following points could be concluded.

For two different rock types, variations in BWI were observed as a function of depth of mining. Specifically, for BGDG rock, a notable increase in ore hardness was observed when the mine depth was below 995 m, followed by a subsequent decrease when the mine level reached a depth below 800 m. In contrast, in GDIR rock, less change was determined, and the average hardness of ore in the elevation range from 815 m to 725 m increased drastically from 17.22 to 18.76 kWh/t. Consequently, future consideration should be given to adjusting the milling circuit at 815 - 725 m depth.

By coupling the ore hardness with the mineralogies, strong correlations between the main mineral phases and the values were found. It was determined that increasing pyrite, muscovite, and quartz content might decrease BWI value. Correlation analysis revealed that albite, orthoclase, and microcline positively correlate with BWI.

The mineral composition (XRD) data were used in setting up the prediction of the BWI estimation model. An equation-based approach to the model for estimating BWI showed a linear correlation with measured BWI. However, the model needs to be validated by numerous BWI tests and mineralogical analyses.

This paper highlights the relationship between

mineralogical composition data and BWI of the BGD and GDIR ores. At Erdenetiin Ovoo Cu-Mo porphyry deposit, the improved knowledge in the geometallurgical characterization and domains of BWI can be used in mine production planning to feed the milling circuit with a relatively homogeneous ore hardness and reduce fluctuations in circuit throughput and energy consumption.

ACKNOWLEDGEMENT

The authors would like to acknowledge the Metallurgical Research and Development Institute of Erdenet Mining Corporation for valuable support in data collection, and experimental work and for providing sample analysis.

Statement of Author Contribution and Conflicts of Interest

B.T. and G.Ch. conceived and supervised the study. B.T., Ch.B., and Ts.Ts. developed the theoretical framework and performed the experiments. D.D., G.D., Kh.A., and N.A. contributed to the interpretation of the results. S.G. and A.D. discussed the results and contributed to the final manuscript. The authors declare no conflicts of interest.

REFERENCES

Adler, J., Parmryd, I. 2010. Quantifying colocalization by correlation: The Pearson correlation coefficient is superior to the Mander's overlap coefficient. *Cytometry Part A*, vol. 77A(8), p. 733-742. <https://doi.org/10.1002/cyto.a.20896>

Ahmadi, R., Shahsavari, S. 2009. Procedure for determination of ball Bond work index in the commercial operations. *Minerals Engineering*, vol. 22(1), p. 104-106. <https://doi.org/10.1016/j.mineng.2008.04.008>

Al-Tigani, M.M.H, Abduealdaem, A.A., Awdekarim, A., Seifelnasr, A.A.S. 2020. Characterization and Bond Work Index Determination of Low Grade Sudanese iron Ore: a case study. *International Journal of Academic Engineering Research*8 vol. 4(5), p. 13-19. <http://ijeais.org/wp-content/uploads/2020/5/IJAER200503.pdf>

Bhukte, P.G., Daware, G.T., Masurkar, S.P., Panchal, M.S., Chaddha, M.J. 2023. Effect of Geological, Mineralogical Characteristics on Grindability of Bauxite: A Case Study of Indian Lateritic Bauxite Deposits. *Journal of the Geological Society of India*, vol. 99(1), p. 55-60. <https://doi.org/10.1007/s12594-023-2266-4>

Bradshaw, D. 2014. The role of 'process mineralogy' in improving the process performance of complex sulphide ores. 20-24 October, IMPC XXVII, Santiago, Chile, p. 24

Dejidmaa G., Kazuki, N. 1998. Previous studies on the Erdenetiin Ovoo porphyry Cu-Mo deposit, Mongolia. *Bulletin of the Geological Survey of Japan*, vol. 49(6), p. 299-308. https://www.gsj.jp/data/bull-gsj/49-06_07.pdf

Dominy, S.C., O'connor, L., Parbhakar-Fox, A., Glass, H.J., Purevgerel, S. 2018. Geometallurgy - A Route to More Resilient Mine Operations. *Minerals*, vol. 8(12), 560. <https://doi.org/10.3390/min8120560>

Frenzel, M., Baumgartner, R., Tolosana-Delgado, R. and Gutzmer, J., 2023. Geometallurgy: present and future. *Elements*, vol. 19(6), pp. 345-351. <https://doi.org/10.2138/gselements.19.6.345>

García, G.G., Oliva, J., Guasch, E., Anticoi, H., Coello-Velázquez, A.L., Menéndez-Aguado, J.M. 2021. Variability study of bond work index and grindability index on various critical metal ores. *Metals*, vol, 11(6), 970. <https://doi.org/10.3390/met11060970>

Gerel, O., Dandar, S., Amar-Amgalan, S., Javkhlanbold, D., Myagamarsuren, Se., Myagamarsuren, Sa., Munkhtsengel, B., Soyolmaa, B. 2005. Geochemistry of granitoids and altered rocks of the Erdenet porphyry copper-molybdenum deposit, Central Mongolia. In Mao J., Bierlein, F.P (Eds) *Mineral Deposit Research: Proceedings of the Eighth Biennial SGA Meeting, Beijing, China, 18 - 21 August 2005*, p. 1137-1140. https://doi.org/10.1007/3-540-27946-6_290

Haruhisa, M. 2003. Geochemical Characteristics of Granitoids of the Erdenet Porphyry Copper Deposit, Mongolia. *Resource Geology*, vol. 53(4), p. 311-316. <https://doi.org/10.1111/j.1751-3928.2003.tb00180.x>

- Hunt, J., Kojovic, T., Berry, R. 2013. Estimating comminution indices from ore mineralogy, chemistry and drill core logging. Conference Proceedings The Second AusIMM International Geometallurgy Conference (GeoMet) 2013. p. 173-176.
- Kalichini, M., Corin, K.C., O'Connor, C.T., Simukanga, S. 2017. The role of pulp potential and the sulphidization technique in the recovery of sulphide and oxide copper minerals from a complex ore. *Journal of the Southern African Institute of Mining and Metallurgy*, vol. 117(8), p. 803-810. <https://doi.org/10.17159/2411-9717/2017/v117n8a11>
- Keeney, L., Walters, S., Kojovic, T. 2011. Geometallurgical mapping and modelling of comminution performance at the Cadia East porphyry deposit. In *GeoMet 2011-1st AusIMM International Geometallurgy Conference*, p. 73-83.
- Kingman, S.W., Jackson, K., Bradshaw, S.M., Rowson, N.A., Greenwood, R. 2004. An investigation into the influence of microwave treatment on mineral ore comminution. *Powder Technology*, vol. 146(3), p. 176-184. <https://doi.org/10.1016/j.powtec.2004.08.006>
- Lessard, J., Sweetser, W., Bartram, K., Figueroa, J., McHugh, L. 2016. Bridging the gap: Understanding the economic impact of ore sorting on a mineral processing circuit. *Minerals Engineering*, vol. 91, p. 92-99. <https://doi.org/10.1016/j.mineng.2015.08.019>
- Magdalinovic, N. 1989. A procedure for Rapid Determination of the Bond work index. *International Journal of Mineral Processing*, vol. 27(1-2), p. 125-132. [https://doi.org/10.1016/0301-7516\(89\)90010-0](https://doi.org/10.1016/0301-7516(89)90010-0)
- Nghipulile, T., Moongo, T.E., Dzinomwa, G., Nkwanyana, S., Mapani, B., Kurasha, J.T. 2022. Evaluation of the Relationship between the Milling Breakage Parameters and Mineralogical Data: A Case Study of Three Copper Ores from a Multi-Mineralised Deposit. *Minerals*, vol. 12(10), 1263. <https://doi.org/10.3390/min12101263>
- Paquot, F.X., Ngulube, C. 2015. Development and optimization of mixed sulphide/oxide copper ore treatment at Kansanshi. *Journal of South African Institute of Mining and Metallurgy*, vol. 115(12), p. 1253-1258. <https://doi.org/10.17159/2411-9717/2015/v115n12a15>
- Parker, T., Shi, F., Evans, C., Powell, M. 2015. The effects of electrical comminution on the mineral liberation and surface chemistry of a porphyry copper ore. *Minerals Engineering*, vol. 82, p. 101-106. <https://doi.org/10.1016/j.mineng.2015.03.019>
- Sarantsatsral, N., Ganguli, R., Pothina, R., Tumen-Ayush, B. 2021. A case study of rock type prediction using random forests: Erdenet copper mine, Mongolia. *Minerals*, vol. 11(10), 1059. <https://doi.org/10.3390/min11101059>
- Saxena, R., Rao, D.P., Gautam, A.K., Gautam, M., Gupta, G.P., Kumar, S., Saxena, V., Singh, C.P., Shankar, V., Gautam, Y. 2024. Correlation Coefficient for Physico-chemical Parameters to Assess the Quality of Tannery Effluents at Kanpur. *Letters in Applied NanoBioScience*, vol. 13(1), 47. <https://doi.org/10.33263/LIANBS131.047>
- Shi, F., Morrison, R., Cervellin, A., Burns, F., Musa, F. 2009. Comparison of energy efficiency between ball mills and stirred mills in coarse grinding. *Minerals Engineering*, vol. 22(7-8), p. 673-680. <https://doi.org/10.1016/j.mineng.2008.12.002>
- Solomon, N., Becker, M., Mainza, A., Petersen, J., Franzidis, J.P. 2011. Understanding the influence of HPGR on PGM flotation behavior using mineralogy. In *Proceedings of the Minerals Engineering*, vol. 24(12), p. 1370-1377. <https://doi.org/10.1016/j.mineng.2011.07.015>
- Todorovic, D., Trumic, M., Andric, L., Milosevic, V., Trumic, M. 2017. A quick method for bond work index approximate value determination. *Physicochemical Problems of Mineral Processing*, vol. 53(1), p. 321-332.
- Varianemil D., Kojovic T., Hakim D., Dilaga R., Condori P. 2023. Ore Hardness Mapping of Batu Hijau Ore Deposit Using the Hardness Index Tester. *Proceedings of the SAG Conference, 2023 Vancouver*.
- Whiteman, E., Lotter, N.O., Amos, S.R. 2016. Process mineralogy as a predictive tool for flowsheet design to advance the Kamao project. *Minerals Engineering*, vol. 96-

97, p. 185-193. <https://doi.org/10.1016/j.mineng.2016.05.004>

Zhou, H., Liu, G., Zhang, L., Zhou, C. 2021. Mineralogical and morphological factors

affecting the separation of copper and arsenic in flash copper smelting slag flotation beneficiation process. *Journal of Hazardous Materials*, vol. 401, 123293.

<https://doi.org/10.1016/j.jhazmat.2020.123293>